Optics-Simplified DSP for 50 Gb/s PON Downstream Transmission using 10 Gb/s Optical Devices

Lei Xue, Lilin Yi, Weisheng Hu, Rui Lin, and Jiajia Chen

***Abstract*—Directly-modulated laser (DML) is widely employed in intensity modulation and direct detection (IMDD) system due to its low cost and high output power. However, the corresponding frequency chirp is regarded as one of the main disadvantages for its application in passive optical networks (PONs). In this paper, we theoretically analyze the frequency response evolution of DML based system under different chirp and dispersion conditions, proving that the system bandwidth can be improved by interactions between negative dispersion and DML chirp. Based on this concept, we experimentally demonstrated downstream 50 Gb/s PAM4 signal transmission over 20 km single-mode fiber (SMF) access based on the 10 Gb/s DML operating at 1310 nm and avalanche photodiode (APD). A dispersion-shifted fiber (DSF) providing −150 ps/nm dispersion at 1310 nm in the optical line terminal (OLT) is used to pre-equalize the frequency response of bandwidth-limited directly modulated signals in the optical domain. Thanks to our proposed dispersion-supported equalization (DSE) technique, the system bandwidth can be improved by 5 GHz. Feed-forward equalization (FFE), decision feedback equalization (DFE) and Volterra filter are employed to evaluate the signal performance improvement, respectively. By evaluating the receiver sensitivity, the DSE combined with FFE scheme shows 2 dB improvement than the complex Volterra algorithm, indicating its potential to reduce the complexity of digital signal processing (DSP) and therefore a lower cost and power consumption in PON.**

***Index Terms*—Digital signal processing (DSP), direct detection, directly modulated laser (DML), dispersion-supported equalization (DSE), passive optical network (PON).**

I. Introduction

USERS requests for ultra-bandwidth services such as 4K/8K online videos, virtual-reality games, and cloud services continue to grow. This global explosive traffic requirement drives data rates of passive optical networks (PONs) to be upgraded towards 100 Gb/s. In 2015, IEEE 100 Gb/s EPON task force was built, with a focus on standardizing a solution for next-generation low-cost 25, 50 and 100 Gb/s PON [1]. Among different solutions, intensity modulation and direct detection (IMDD) has been adopted as the mainstream technology in next generation PON systems. At the earlier stage of standardization discussion, improving the single wavelength capacity from 10 Gb/s to 25 Gb/s was the research focus [2], [3]. By multiplexing two or four wavelengths, 50 Gb/s or 100 Gb/s system capacity can be achieved [4]. However, only 2.5 times capacity improvement per wavelength is a small step compared with the upgrades occurred in the previous generations (e.g., four times capacity improvement from 2.5 Gb/s EPON to 10 Gb/s EPON). Moreover, the optical spectrum is the most valuable resource in optical communication systems, four-wavelength multiplexing achieving 100 Gb/s is not cost-effective. Then 50 Gb/s time division multiplexing (TDM)-PON was proposed as an alternative [5], which was typically realized by using high order modulation formats to increase the bandwidth efficiency and therefore reduce the requirement for devices' bandwidth [6], [7]. Recently, 50 Gb/s electrical duo-binary (EDB) and 4 pulse amplitude modulation (PAM4) transmission over 20 km single-mode fiber (SMF) have been demonstrated, in which 25 Gb/s electro-modulated laser (EML) and avalanche photodiode (APD) are used in the system [6]. Until now, 25 Gb/s optical devices especially APD are still costly for the real deployment of EPON. Leveraging mature 10 Gb/s components combined with digital signal processing (DSP) is a favorable option [8], [9]. In [9], 50 Gb/s PAM4 and discrete multi-tone (DMT) transmission over 20 km SMF based on 10 Gb/s directly-modulated laser (DML) and APD in O-band has been achieved, where off-line electrical feed-forward equalization (FFE) and maximum likelihood sequence estimation (MLSE) algorithms are employed for channel equalization. The main disadvantage of using digital equalizer at receiver side is the enormous power consumption due to the high computational complexity in optical network unit (ONU). To solve this problem, electrical pre-equalization in the optical line terminal (OLT) side is proposed, which allows a high sharing factor [10], [11]. Apart from this solution, optical signal processing in the OLT side can also improve the quality of the bandwidth-limited signal to reduce the complexity of DSP at the ONU side. In [12], by using the interplay between DML adiabatic chirp and fiber dispersion, the frequency notch of the SMF is compensated. 51.56 Gb/s non-return-to-zero on-off keying (NRZ-OOK) signal transmission based on 20 Gb/s C-band DML and photodiode (PD) is achieved. In our previous

Manuscript received April 29, 2019; revised August 7, 2019; accepted September 12, 2019. Date of publication September 19, 2019; date of current version February 1, 2020. This work was supported in part by the National Natural Science Foundation of China under Grant 61575122, and in part by the EU H2020 5G STEP-FWD under Grant 722429. *(Corresponding author: Lilin Yi.)*

L. Xue is with the State Key Lab of Advanced Optical Communication Systems and Networks, Shanghai Institute for Advanced Communication and Data Science, Shanghai Jiao Tong University, Minhang 200240, China, and also with the Chalmers University of Technology, 412 96 Göteborg, Sweden (e-mail: leixue@sjtu.edu.cn).

L. Yi and W. Hu are with the State Key Lab of Advanced Optical Communication Systems and Networks, Shanghai Institute for Advanced Communication and Data Science, Shanghai Jiao Tong University, Minhang 200240, China (e-mail: lilinyi@sjtu.edu.cn; wshu@sjtu.edu.cn).

R. Lin and J. Chen are with the Chalmers University of Technology, 412 96 Göteborg, Sweden (e-mail: rulin@kth.se; jiajiac@kth.se).

Color versions of one or more of the figures in this article are available online at http://ieeexplore.ieee.org.

Digital Object Identifier 10.1109/JLT.2019.2942438

work [13], we realized 25 Gb/s NRZ-OOK signal transmission based on 10 Gb/s optical devices, where the introduced negative dispersion and positive chirp of DML are effectively interacted to equalize the bandwidth rather than using DSP. Therefore, simple optical signal processing can be considered to reduce the complexity of DSP algorithms needed at the ONUs, which is referred to as optics-simplified DSP (OsDSP) solution.

This paper is an extension of our previous work [14]. Based on the concept of OsDSP, we propose to exploit using negative dispersion in the PON which deploys low bandwidth transceiver based DML-based direct modulation and direct detection (DML/DD) system to reduce the complexity of the DSP needed at ONUs, and therefore reduce the power consumption as well. To verify the frequency equalization effect of negative dispersion, we experimentally demonstrate O-band 50 Gb/s PAM4 PON over a 20 km SMF based on 10 Gb/s DML and APD. A span of 10 km dispersion-shifted fiber (DSF) with around -150 ps/nm dispersion at 1310 nm is used to improve the system 3 dB bandwidth from 6 GHz to 11 GHz. To further enhance the signal quality, FFE/DFE, Volterra filters are employed for off-line equalization. An O-band semiconductor optical amplifier (SOA) is employed to compensate for the insertion loss of DSF and improve the system power budget. Enabled by the dispersion-supported equalization (DSE) technique, a 15-tap FFE filter is enough for inter-symbol interference (ISI) elimination targeting 2×10^{-2} bit error rate (BER) threshold. Compared to the complex Volterra filter, the DSE-assisted simple FFE filter achieves 2 dB improvement of receiver sensitivity, which proves the concept of OsDSP. Moreover, with the help of the OsDSP, a power budget of 26 dB is achieved. The main contributions of this paper are: 1) we provide intensive theoretical analyses on the effects of transient and adiabatic chirps on a DML/DD transmission system with both positive and negative dispersion; 2) we carry out simulation demonstrating that negative dispersion can effectively improve bandwidth of the system; and 3) we implement experiment to validate the system performance improvement in terms of end-to-end system bandwidth, BER, receiver sensitivity and power budget.

II. Principle

To clarify the bandwidth evolution in the end-to-end DML/DD system with different dispersion, we derivate the frequency response function of the whole system. The small-signal response of the DML can be denoted as [15]

$$S_{\mathrm{in}}(jw) = H(jw)\, I_{in}(jw) \tag{1}$$

$$H(jw) = \frac{{w_0}^2}{w_0^2 + jw\Gamma - w^2} \tag{2}$$

where $H(jw)$ is the modulation transfer function, $I_{in}(jw)$ is the modulated signal, w_0 is the relaxation oscillation frequency, and Γ is the damping rate.

Due to the complex susceptibility of the gain medium in the DML, frequency modulation (FM) is induced simultaneously with the amplitude modulation (AM). The relation between the instantaneous frequency shift $\Delta\nu$ and the optical power P can be expressed as [16]

$$\Delta\nu = \frac{1}{2\pi}\frac{d\varphi}{dt} = \frac{\alpha}{4\pi}\left(\frac{1}{P}\frac{dP}{dt} + \kappa P\right) \tag{3}$$

where α is the linewidth enhancement factor and κ is the adiabatic chirp factor. The first term stands for the transient chirp, and the second term expresses the adiabatic chirp.

The response of the partial conversion from AM to FM can be described by

$$F_{in}(jw) = \frac{\alpha}{2}(jw + \Gamma)\frac{1}{P_0}S_{in}(jw) \tag{4}$$

where P_0 is the average output power of the laser before modulation. During the SMF transmission, AM and FM partially convert to each other because of the interplay between the chirp and dispersion. The transfer matrix between them can be expressed as

$$\begin{pmatrix} S_{out}(jw) \\ F_{out}(jw) \end{pmatrix} = \begin{pmatrix} \cos(w^2\theta) & \frac{2jP_0\sin(w^2\theta)}{w} \\ \frac{jw\sin(w^2\theta)}{2P_0} & \cos(w^2\theta) \end{pmatrix} \cdot \begin{pmatrix} S_{in}(jw) \\ F_{in}(jw) \end{pmatrix} \tag{5}$$

where θ is given as $D\lambda^2 w^2 l/4\pi c$, D is the fiber dispersion parameter, λ is the wavelength of the optical signal, l is the fiber length, and c is the speed of light in vacuum.

Substituting (4) into (5), we can obtain the frequency response of the fiber by

$$\begin{aligned} G(jw) &= S_{\mathrm{out}}(jw)/S_{\mathrm{in}}(jw) \\ &= \sqrt{1+\alpha^2}\cos(\theta + \mathrm{arc}\tan(\alpha)) + j\frac{\alpha\kappa P_0}{w}\sin(\theta) \end{aligned} \tag{6}$$

The first and the second terms in (6) reflects the transient and adiabatic chirp of the DML, respectively. If the adiabatic chirp factor κ is zero, the dispersion-induced power fading of (6) becomes $\sqrt{(1+\alpha^2)}\cos(\theta + \mathrm{arc}\tan(\alpha))$, which is the case in an EML- or MZM-based system [17]. For a chirp-free signal, the frequency response of fiber becomes $\cos(\theta)$ [18].

Based on (6), we first investigate the frequency response under three different chirp settings: 1) without chirp, i.e., $\alpha = 0$, $\kappa = 0$; 2) only with transient chirp, i.e., $\alpha = 3.5$, $\kappa = 0$; and 3) with both transient and adiabatic chirp factor $\alpha = 3.5$, $\kappa = 13$ GHz/mW. The dispersion value is set as 320 ps/nm, which is the aggregated dispersion of a 20 km SMF at 1550 nm. Since both positive and negative dispersion can be generated in C-band, 1550 nm is selected here for simulation. The theoretical dispersion induced power fading under the settings are plotted in Fig. 1(a). The frequency response shows a low-pass filtering character owing to the feature of the cosine function in (6). With absence of the chirp (as the green line shows), the first notch induced by the fiber dispersion appears at around 15 GHz. However, this notch moves to 6 GHz as the transient chirp is introduced in the transmitted signal, resulting in serious degradation of the

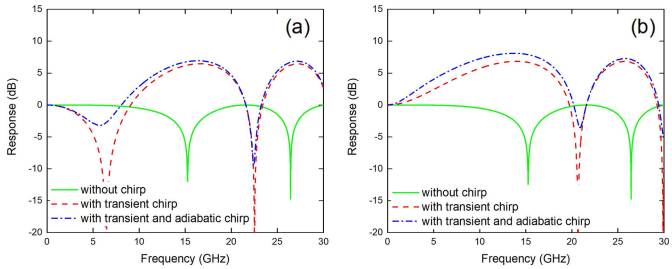

Fig. 1. Theoretically calculated frequency response curves of SMF. (a) With 320 ps/nm. (b) -320 ps/nm dispersion at 1550 nm.

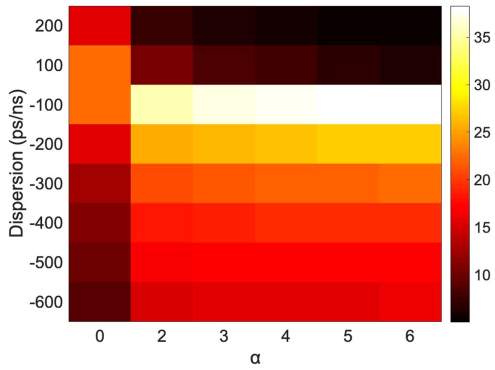

Fig. 2. Theoretically calculated 3 dB bandwidth evaluation of the fiber at different dispersion and transient chirp factor.

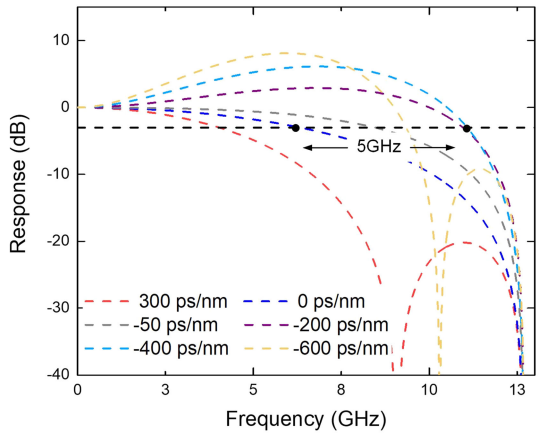

Fig. 3. Theoretically calculated frequency response curves of the end-to-end system with 10 Gb/s transceivers and varied chromatic dispersion.

high-frequency components. When adiabatic chirp is induced (see the blue dash), the first notch can be alleviated due to the sine-like frequency response, which means that adiabatic chirp can provide power gain to smooth the first power dip. Based on this phenomenon, several works have been done achieving high-speed long-reach transmission using the DML [12], [19]. However, when κ and P_0 are small, the power gain provided by adiabatic chirp is not enough to compensate the dip completely.

On the other hand, if the negative dispersion is applied, the results are quite different. Based on the same chirp setting, Fig. 1(b) shows the frequency response of the fiber with a dispersion of -320 ps/nm. The frequency response curve of the fiber without any chirp is the same with the case in Fig. 1(a). However, the first dip of the power fading moves to $\sim$ 20 GHz when the transient chirp is induced and the power at the high frequency part is improved due to the transfer of FM to AM. With the help of the adiabatic chirp, the power gain at the notch can be further improved.

Based on the above results, we can infer that when the high-speed signal is directly modulated and detected by bandwidth-limited optical components, the first notch induced by the first term of (6) can be moved to the higher frequency part by employing the negative dispersion, and the distorted high-frequency components due to the bandwidth-limited optics can be partially compensated by the power gain. Therefore, bandwidth equalization can be achieved by transferring phase modulation into intensity modulation. To evaluate the flexibility of the proposed equalization technique, we need to consider the equalization performance under different chirp and negative dispersion values.

The transient chirp is related to the linewidth enhancement factor α, and the bandwidth improvement dependence on this value needs to be evaluated. Notably, α and κ of commercial DMLs are typically 2–6 and 10–15 GHz/mW [20], respectively. Fig. 2 shows the 3 dB bandwidth of the fiber link at different dispersions and transient chirps. For this evaluation, the output power of DML is 8 dBm, κ is 13 GHz/mW. Sufficient bandwidth of optoelectronic devices is considered here. It can be observed that when positive dispersion exists in the system, the 3 dB bandwidth decreases as the transient chirp and the dispersion amount increases. This is because the power notch induced by the transient chirp moving towards the lower frequency part. The results are inverted when the dispersion changes to be negative. The improvement of 3 dB bandwidth varies with the transient chirp values resulting from the different power gains. However, compared with the case without any chirp (i.e., $\alpha = 0$), the bandwidth can always be improved with little fluctuation in the whole range of α from 2 to 6 at the fixed dispersion, which means the optics assisted bandwidth improvement is insensitive to commercial optical links deploying DMLs with different chirp characteristics. Regarding the relationship between dispersion value and bandwidth improvement, when the negative dispersion value is within -200 ps/nm, more than 10 GHz bandwidth improvement can be achieved. With the increase of negative dispersion value, the improvement decreases gradually. In the practical implementation, the bandwidth limitation from the optoelectronic devices also influences the performance, which has been elaborated in the following paragraph.

To evaluate the relation between system bandwidth and the dispersion in a practical case, a low-pass filter with 3-dB bandwidth of 6 GHz is added to simulate the 10 Gb/s transceiver-based system. Here, α and κ are fixed to 3.5 and 13 GHz/mW, respectively. The results are shown in Fig. 3. The blue dashed curve corresponding to 0 ps/nm case shows the amplitude response in back-to-back (BtB) case. When the positive dispersion is applied, the bandwidth decreases as the dispersion increases, which is the same as the previous analysis. As the dispersion changes from 0 to -200 ps/nm, the 3 dB system bandwidth can

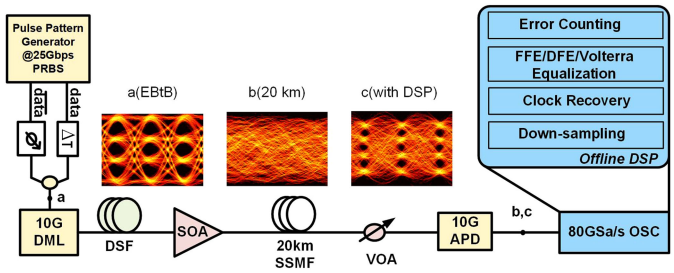

Fig. 4. Experimental setup. (a) Electrical eye diagram at the input of the DML and eye diagrams after 20km. SMF transmission. (b) Without DSP. (c) With DSP.

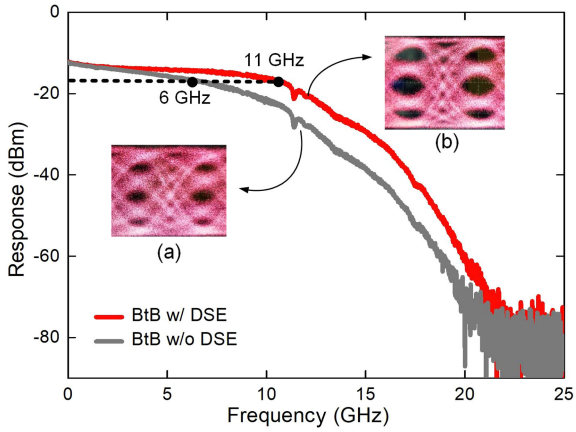

Fig. 5. Measured frequency response of a 10 Gb/s DML and APD based system at BtB with and without DSE. Inset: Optical eye-diagram of 25 Gb/s PAM-4 signal. (a) without DSE. (b) with DSE.

be improved from 6 GHz to 11 GHz. With the further increase of the negative dispersion, the frequency response becomes less flat, while the 3 dB bandwidth is almost the same. When the dispersion reaches to −600 ps/nm, the frequency notch appears and results in decreased system bandwidth. Considering the 3 dB system bandwidth and the flatness of the response, the optimal compensation range is around −200 ps/nm.

III. Experimental Setup and Results

Fig. 4 shows the experimental setup for the performance evaluation of our proposed 50 Gb/s/λ downstream transmission in TDM-PON. At the OLT side, we use a pulse pattern generator (PPG, Keysight N4960A) to generate 50 Gb/s PAM4 signal. By manipulating the amplitude and delay, two 25 Gb/s pseudo-random bit sequence (PRBS) with $2^{15}-1$ in length are combined by 50 GHz coupler, generating an electric 50 Gb/s PAM4 signal with 1.5 V peak-to-peak power. The corresponding eye diagram is shown in inset (a). Since O-band is more favorable for downstream 50 G-PON in recent 100 G EPON standardization discussion, a 10 Gb/s DML operating at ∼1310 nm is employed to convert the electrical signal into the optical domain. The α and κ of this DML are 3.8 and 12 GHz/mW respectively. To pre-compensate the bandwidth, the generated optical signal is launched to a reel of 10 km DSF with a dispersion of −150 ps/nm at 1310 nm and an insertion loss of 10 dB. Note that other components with negative dispersion in O-band can also be used. To increase the power budget, an O-band SOA (Inphenix IPSAD 1316c) is used to boost the launch power to the 20 km SMF. The SOA has a small-signal gain of 22 dB, noise figure of 6.8 dB and saturation output power of 10 dBm. Both DSF and SOA are used at the OLT side, where the cost can be shared by all connected users. After 20 km SMF transmission, a variable optical attenuator (VOA) is employed to emulate the power loss by the optical splitter and vary the optical signal power for receiver sensitivity measurements. At the receiver side, a 10 Gb/s APD with a 3 dB bandwidth of 7 GHz is used to directly detect the optical signal and convert it to the electrical signal. The received electrical signal is first sampled by a Keysight real-time oscilloscope (DSOV334A) with a sampling rate of 80 GSa/s and then processed offline in Matlab. In the offline DSP part, the captured PAM4 signal is firstly re-sampled, synchronization, and normalized. Then, FFE, DFE and Volterra filters are applied to mitigate the signal distortions due to the bandwidth limitation induced ISI. The FFE, DFE taps and Volterra kernels are updated by least mean square (LMS) algorithm.

From the analysis in Section II, we know that the 3 dB bandwidth of a 10 Gb/s DML based transmission system can be increased by 5 GHz when an amount of negative dispersion is employed. To prove this effect, we first measure the frequency response of the system composed of 10 Gb/s O-band DML and APD at BtB case. The results are shown in Fig. 5, where we can see the high-frequency response is improved significantly leading to the 3 dB end-to-end system bandwidth increase from 6 GHz to 11 GHz. It is consistent with the simulation results. To demonstrate whether the DSE technology works efficiently with signal modulation, we measure the eye diagrams of 25 Gb/s PAM signal at BtB case shown in insets of Fig. 5. It can be observed that the eye diagram is less open in inset (a) due to the bandwidth limitation compared to the case after employing the DSE. However, when the data rate is up to 50 Gb/s, the eye diagram, which is shown in inset (b) of Fig. 4, is completely closed after 20 km transmission because the bandwidth improvement by DSE is insufficient for such high data rate transmission. Electrical equalization technique is required to further reduce the linear and non-linear ISI distortion. After equalized by off-line DSP, signal quality is greatly improved and the eye diagram turns to open, as shown in inset (c) of Fig. 4.

As explained in Section II, the system bandwidth improvement originates from the interaction between the chirp and negative dispersion. From (3), we know that the chirp value of the DML varies with the output power. On the other hand, to obtain optimal signal-to-noise ratio (SNR), the DML also needs to be biased at the linear regime. Low bias current relates to small chirp, which may not be optimal for DSE, while high bias current is not suitable for PAM4 modulation. To find the optimal bias current, we measure the output power of DML and evaluate the receiver sensitivity of 50 Gb/s PAM4 signal at BtB by tuning the operating current of DML. The modulation amplitude is fixed to 1.5 V and 30-tap FFE is used for bandwidth equalization. The receiver sensitivity is defined as the received optical power

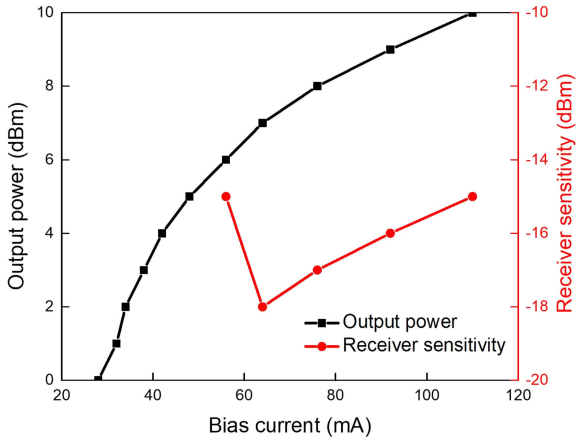

Fig. 6. DML Output power and 50 Gb/s PAM4 signal receiver sensitivity at different bias current.

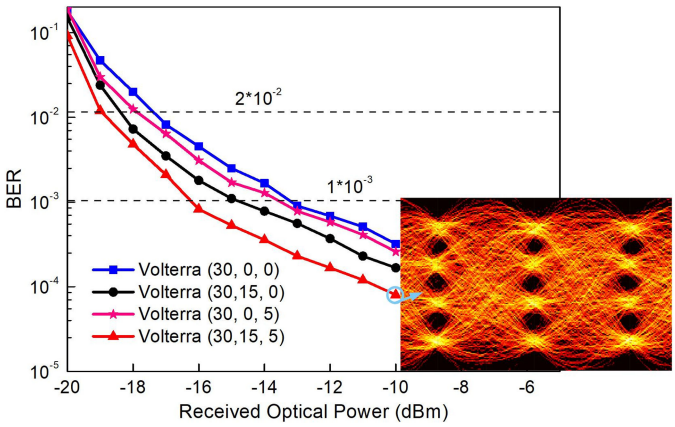

Fig. 8. Measured BER performances of 50 Gb/s PAM-4 signal with different Volterra memory length after 20 km with DSE.

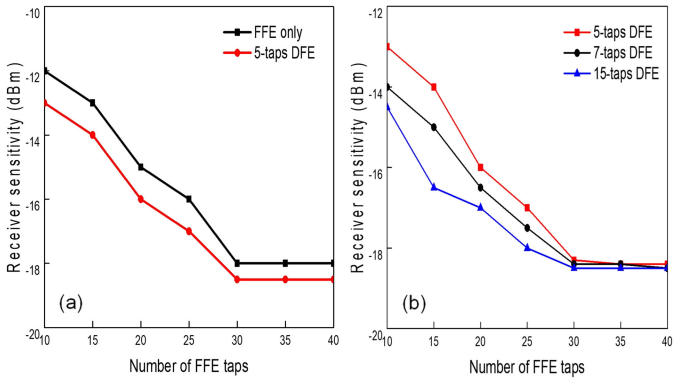

Fig. 7. Receiver sensitivity after 20 km SMF transmission as a function of FFE and DFE filter taps at BER of 2×10^{-2}. (a) FFE only vs FFE + DFE-5. (b) Different taps of DFE and FFE.

at the Soft-decision low-density parity check (SD-LDPC) BER threshold of 2×10^{-2} [21]. The results are shown in Fig. 6. The best receiver sensitivity presents when the bias current is around 60 mA with 7 dBm output power. This bias point also locates at the linear regime of output power vs. bias current curve. In the following tests, we fix the operating point of the DML at this state.

BER cannot be measured without off-line equalization due to the eye diagram is completely closed even with DSE shown in the inset (b) of Fig. 4. We first employ simple FFE and DFE filter to equalize the signal. Fig. 7 shows the performance assessment of equalizers with a different number of taps in both FFE and DFE filter after 20 km transmission. 15-taps FFE can achieve a sensitivity of -13 dBm, and the sensitivity improves with the increase of FFE taps, as shown in Fig. 7(a). The receiver sensitivity achieves -18 dBm with 30 taps and a further increase of the taps makes negligible improvement. Then we add 5 taps DFE to further compensate the ISI, only $\sim$0.5 dB improvement can be obtained. Similar to FFE, the receiver sensitivity improves with the increase of DFE taps, but once the FFE taps is beyond 30, negligible improvement can be observed.

For the PAM4 based DML/DD system, except for linear distortion, modulators and detectors also induce nonlinear distortion. Volterra filter is a universal equalizer to mitigate the linear and nonlinear distortion [22]. To further improve the receiver sensitivity, we employ three kernels Volterra filter to compensate for the nonlinear degradation in the system. Note that the memory length of the kernel is defined as Volterra (L1, L2, L3) in Fig. 8. We compare four cases with different memory lengths of Volterra kernels after 20 km with DSE. The receiver sensitivity is improved from -13 dBm to -16 dBm at the BER threshold of 1×10^{-3} when the memory length of Volterra kernel increase from (30, 0, 0) to (30, 15, 5) shown in Fig. 8. However, when the received optical power is lower than -18 dBm, only $\sim$1 dB receiver sensitivity improvement at the BER of 2×10^{-2} can be obtained, we attribute this to the poor SNR of the signal. Same as FFE, the Volterra filter also increase noise power during equalization, more kernels do not provide further improvement except for higher computation complexity. We can also observe that the Volterra equalizer with only first- and second-order kernel performs better than that with first- and third-order kernels, which means that the second-order nonlinearity is more severe than the third-order nonlinearity in the DML/DD system.

Fig. 9 shows the BER curves of 50 Gb/s PAM4 signal transmission over a 20 km SMF using three different equalization configurations. Without DSE for pre-equalization, applying Volterra (30 15 5) filter can only achieve -16 dBm receiver sensitivity at the BER of 2×10^{-2}. After DSE is employed, 3 dB receiver sensitivity improvement can be obtained with the same number of Volterra kernels. In this case, 30-taps FFE filter is able to achieve -18 dBm receiver sensitivity with 2 dB sensitivity improvement. To evaluate the computation complexity between these two filters, we compare the number of real multipliers for tap updating by LMS to obtain one symbol output from the filter. For the three-order Volterra (30 15 5) filter, the total number of multiplications for tap updating is 185, while the 30-tap FFE filter only requires 30 multipliers [23]. Therefore, 2 dB receiver sensitivity improvement as well as reduced computation complexity are obtained after employing DSE technique.

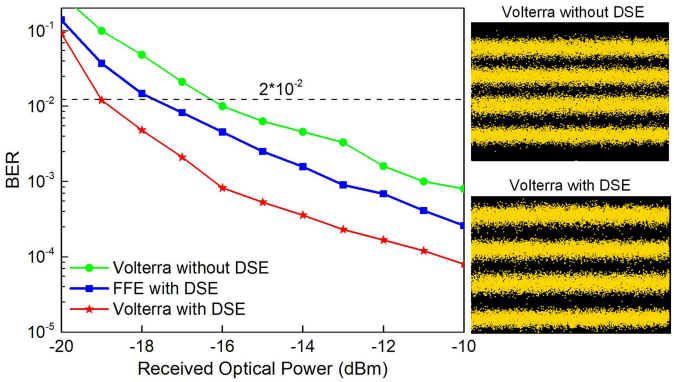

Fig. 9. BER performances of 50 Gb/s PAM4 signal transmission over 20-km SMF for different equalization configurations.

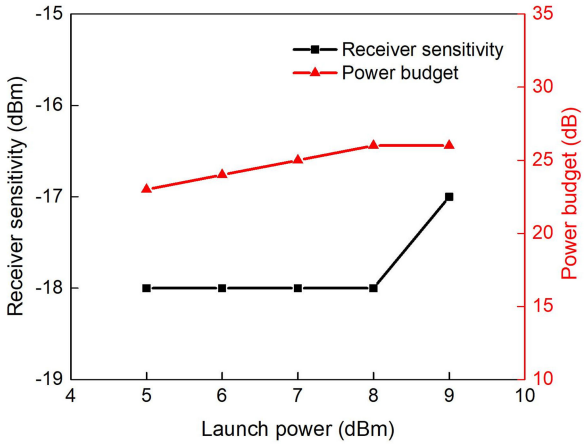

Fig. 10. Required optical power over 20 km SMF for a BER of 2×10^{-2} versus launch power.

Finally, to exploit the advantage of our system for the downstream, we investigate the dependence of required launch power for 20 km transmission reaching BER of 2×10^{-2} in the equalization case of DSE-assisted FFE. To avoid gain saturation effect of the SOA, an optical attenuator is used before the SOA to lower the input power to −10 dBm. The final results are shown in Fig. 10. It can be observed that the optimal output power of SOA is 8 dBm and the corresponding loss budget is 26 dB which is able to meet the PR-20 with 24 dB power budget requirement. Higher launch power adds more nonlinear distortions to the signal, and then the receiver sensitivity and corresponding power budget turns to degrade.

IV. Conclusion

In this paper, we have experimentally demonstrated a dispersion-assisted DML/DD PON system with 50 Gb/s PAM4 signal transmission over a 20 km SMF based on O-band 10 Gb/s DML and APD. DSF with negative dispersion is employed at the transmitter side to pre-equalize the limited bandwidth in the optical domain so as to reduce the complexity of DSP. Compared to the pure Volterra filter, the DSE-assisted FFE filter can achieve 2 dB improvement of receiver sensitivity as well as reduced computation complexity. With the help of SOA, the insertion loss of DSF can be fully compensated and the launch power is optimized, realizing a 26 dB power budget. Our results verify that introducing optic signal processing is able to simplify DSP complexity at reception, providing an alternative to use low-bandwidth devices to achieve high data rate PONs. Besides O-band, such a scheme can also be applied to other wavelength bands, in which the mismatch between the induced negative dispersion, fiber dispersion and chirp effect needs to be well considered. Such a concept is beneficial for access networks that are cost- and energy-sensitive.

References

[1] V. Houtsma, D. V. Veen, and E. Harstead, "Recent progress on standardization of next generation 25, 50 and 100G EPON," *J. Lightw. Technol.*, vol. 35, no. 6, pp. 1228–1234, Mar. 2017.

[2] D. T. van Veen and V. E. Houtsma, "Symmetrical 25-Gb/s TDM-PON with 31.5-dB optical power budget using only off-the-shelf 10-Gb/s optical components," *J. Lightw. Technol.*, vol. 34, no. 7, pp. 1636–1642, Apr. 2016.

[3] J. Man, S. Fu, H. Zhang, J. Gao, L. Zeng and X. Liu, "Downstream transmission of pre-distorted 25-Gb/s faster than-Nyquist PON with 10G-class optics achieving over 31 dB link budget without optical amplification," in *Proc. Opt. Fiber Commun. Conf. Exhib.*, Anaheim, CA, USA, 2016.

[4] H. Ji *et al.*, "Field demonstration of a real-time 100-Gb/s PON based on 10G-class optical devices," *J. Lightw. Technol.*, vol. 35, no. 10, pp. 1914–1921, May 2017.

[5] D. Lavery *et al.*, "Opportunities for optical access network transceivers beyond OOK," *J. Opt. Commun. Netw.*, vol. 11, no. 2, pp. A186–A195, Feb. 2019.

[6] V. Houtsma, and D. V. Veen, "Bi-directional 25G/50G TDM-PON with extended power budget using 25G APD and coherent detection," *J. Lightw. Technol.*, vol. 36, no. 1, pp. 122–127, Jan. 2018.

[7] M. Huang *et al.*, "Cost-effective 25G APD TO-Can/ROSA for 100G applications," in *Proc. Opt. Fiber Commun. Conf. Exhib*, Los Angeles, CA, USA, 2017.

[8] X. Tang *et al.*, "Equalization scheme of C-band PAM4 signal for optical amplified 50-Gb/s PON," *Opt. Express*, vol. 26, no. 25, pp. 33418–33427, 2018.

[9] M. Tao, L. Zhou, H. Zeng, S. Li, and X. Liu, "50-Gb/s/λ TDM-PON based on 10G DML and 10G APD supporting PR10 link loss budget after 20-km downstream transmission in the O-Band," in *Proc. Opt. Fiber Commun. Conf. Exhib*, Los Angeles, CA, USA, 2017.

[10] J. Zhang *et al.*, "Symmetrical 50-Gb/s/λ PAM-4 TDM-PON in O-band with DSP and semiconductor optical amplifier supporting PR-30 link loss budget," in *Proc. Opt. Fiber Commun. Conf. Exhib*, San Diego, CA, USA, 2018.

[11] K. Zhang *et al.*, "Design and analysis of high-speed optical access networks in the O-band with DSP-free ONUs and low-bandwidth optics," *Opt. Express*, vol. 26, pp. 27873–27884, 2018.

[12] S. H. Bae, H. Kim, and Y. C. Chung, "Transmission of 51.56-Gb/s OOK signal using 1.55μm directly modulated laser and duobinary electrical equalizer," *Opt. Express*, vol. 24, no. 20, pp. 2555–22562, 2016.

[13] L. Xue, L. Yi, H. Ji, P. Li, and W. Hu, "Symmetric 100-Gb/s TWDM-PON based on 10G-class optical devices enabled by dispersion-supported equalization," *J. Lightw. Technol.*, vol. 36, no. 2, pp. 580–586, Jan. 2018.

[14] L. Xue, L. Yi, P. Li, and W. Hu, "50-Gb/s TDM-PON based on 10G-class devices by optics-simplified DSP," in *Proc. Opt. Fiber Commun. Conf. Exhib.*, San Diego, CA, USA, Mar. 2018.

[15] J. M. Wang and K. Petermann, "Small-signal analysis for dispersive optical fiber communication-systems," *J. Lightw. Technol.*, vol. 10, no. 1, pp. 96–100, Jan. 1992.

[16] L. Bjerkan, A. Royset, L. Hafskjer and D. Myhre, "Measurement of laser parameters for simulation of high-speed fiber optic systems," *J. Lightw. Technol.*, vol. 14, no. 5, pp. 839–850, May 1996.

[17] D.-Z. Hsu, C.-C. Wei, H.-Y. Chen, W.-Y. Li, and J. Chen, "Cost-effective 33-Gbps intensity modulation direct detection multi-band OFDM LR-PON system employing a 10-GHz-based transceiver," *Opt. Express*, vol. 19, no. 18, pp. 17546–17556, 2011.

[18] U. Gliese, S. Nørskov, and T. N. Nielsen, "Chromatic dispersion in fiber-optic microwave and millimieter-wave links," *IEEE Trans. Microw. Theory Techn.*, vol. 44, no. 10, pp. 1716–1724, Oct. 1996.
[19] C.-C. Wei, "Small-signal analysis of OOFDM signal transmission with directly modulated laser and direct detection," *Opt. Lett.*, vol. 36, no. 2, pp. 151–153, 2011.
[20] C. Wei, "Analysis and iterative equalization of transient and adiabatic chirp effects in DML-based OFDM transmission systems," *Opt. Express*, vol. 20, no. 23, pp. 25774–25789, 2012.
[21] L. Li, X. Liu and F. Effenberger, "Soft-decision LDPC for 50G-PON," in *Proc. D75, ITU-T Q2 Interim Meet.*, 2018.
[22] F. P. Guiomar, J. D. Reis, A. L. Teixeira and A. N. Pinto, "Digital post compensation using Volterra series transfer function," *IEEE Photon. Technol. Lett.*, vol. 23, no. 19, pp. 1412–1414, Oct. 2011.
[23] K. Zhong *et al.*, "Experimental study of PAM-4, CAP-16, and DMT for 100 Gb/s short reach optical transmission systems," *Opt. Express*, vol. 23, pp. 1176–1189, 2015.

Lei Xue received the B.S. degree in communication engineering from the School of Information Science and Engineering, Hunan University, Hunan, China, in 2015. He is currently working toward the Ph.D. degree in the Future Ready Optical Network Technology Research Group, State Key Laboratory of Advanced Optical Communication Systems and Networks, Shanghai Jiao Tong University, Shanghai, China. His research interests include optical access network and short reach optical interconnection.

Lilin Yi received the Ph.D. degree from the Ecole Nationale Supérieure des Télécommunications (ENST, currently named as Telecom ParisTech), France and SJTU, China, in March and June 2008, respectively, as a joint-educated Ph.D. student. Currently he is a Full Professor with the Shanghai Jiao Tong University, Shanghai, China. He is the author or co-author of more than 180 papers in peer-reviewed journals and conferences, including invited papers/talks in JLT/OFC/ECOC. His main research topics include high-speed optical communications, optical signal processing, and machine learning based-digital signal processing.

Dr. Yi serves as the TPC member and workshop organizer for a number of international conferences including OFC, ECOC, OECC, CLEO-PR, and ACP. He is an associate editor of *Optical Fiber Technology*, and a guest editor of *Applied Science*. He has achieved the awards of "Young scholars of the Yangtze River in China", and "National Science Fund for Excellent Young Scholars of China".

Weisheng Hu received the B.Sc., M.Eng., and Ph.D. degrees from Tsinghua University, Beijing, China, University of Science and Technology Beijing, Beijing, China, and Nanjing University, Nanjing, China, in 1986, 1989, and 1997, respectively. He joined Shanghai Jiao Tong University as a Postdoctorate Fellow, from 1997, and as a Professor from 1999, where he was promoted to Distinguished Professor in 2009. He served as the Deputy Director and Director of State Key Laboratory of Advanced Optical Communication Systems and Networks, during 2002 and 2012. He has published about 300 peer-reviewed journal/conference papers.

Dr. Hu serves in five editorial boards including *Optics Express*, JOURNAL OF LIGHTWAVE TECHNOLOGY, *Chinese Optics Letters*, and *China Communications*. Also he served in program committees of a number of international conferences, including OFC, ICC, Globecom, INFOCOM, OPTICS-East, ACP, etc.

Rui Lin received the Ph.D. degree in Communication Systems from KTH Royal Institute of Technology in 2016. Since 2019, she has worked as a Postdoctoral Researcher at CTH. Her research interests include high capacity optical communication network and quantum communication. She has authored and co-authored more than 30 journal and conference papers. She has been involved in multiple national research projects.

Dr. Lin is a regular reviewer for several IEEE, OSA, and SPIE journals.

Jiajia Chen received the Ph.D. degree and Docent degree in 2009 and 2015 from KTH Royal Institute of Technology, respectively. Currently, she is a Professor with the Department of Electrical Engineering at Chalmers University of Technology, Göteborg, Sweden. She has 80+ peer-reviewed articles published in the leading international journals, 120+ conference papers (30+ invited talks/tutorials), 1 book, 7 book chapters and 10 patent applications. Over the last decade, her research broadly has concerned optical communications and networks, addressing various aspects including cybersecurity, resource utilization, capacity, energy efficiency and cost efficiency.

Dr. Chen is a Principal Investigator of several individual and collaborative research projects funded by the Swedish Foundation of Strategic Research (SSF), Göran Gustafssons Foundation, and Swedish Research Council (VR), demonstrating her strong ability to secure and manage external funding. Because of her excellent research work in supporting 5G and cloud environment, she received "Göran Gustafssons Stora Pris till Yngre Forskare" in 2015, which is a prize for young Swedish researchers at age below 36.